

CERN-EP-2022-200  
21 September 2022

# Observation of a resonant structure near the $D_s^+ D_s^-$ threshold in the $B^+ \rightarrow D_s^+ D_s^- K^+$ decay

LHCb collaboration

## Abstract

An amplitude analysis of the  $B^+ \rightarrow D_s^+ D_s^- K^+$  decay is carried out to study for the first time its intermediate resonant contributions, using proton-proton collision data collected with the LHCb detector at centre-of-mass energies of 7, 8 and 13 TeV. A near-threshold peaking structure, referred to as  $X(3960)$ , is observed in the  $D_s^+ D_s^-$  invariant-mass spectrum with significance greater than 12 standard deviations. The mass, width and the quantum numbers of the structure are measured to be  $3956 \pm 5 \pm 10$  MeV,  $43 \pm 13 \pm 8$  MeV and  $J^{PC} = 0^{++}$ , respectively, where the first uncertainties are statistical and the second systematic. The properties of the new structure are consistent with recent theoretical predictions for a state composed of  $c\bar{c}s\bar{s}$  quarks. Evidence for an additional structure is found around 4140 MeV in the  $D_s^+ D_s^-$  invariant mass, which might be caused either by a new resonance with the  $0^{++}$  assignment or by a  $J/\psi\phi \leftrightarrow D_s^+ D_s^-$  coupled-channel effect.

Submitted to Phys. Rev. Lett.



Exotic hadrons<sup>1</sup> play a crucial role in studies of Quantum Chromodynamics (QCD), and provide a unique window to understand the nature of the strong force. Dozens of charged exotic states with hidden charm or beauty, which imply multi-quark nature, such as  $Z_c(4430)^+$  [1, 2],  $Z_b(10610)^+$  [3],  $Z_c(3900)^+$  [4–6],  $Z_c(4020)^+$  [7, 8],  $P_c(4450)^+$  [9, 10],  $Z_{cs}(3985)^+$  [11],  $Z_{cs}(4000)^+$  [12], have been recently discovered by various experiments.<sup>2</sup> Over the last two years, the LHCb collaboration reported three new open-charm tetraquark states,  $X_{0,1}(2900)^0$  [13, 14] and  $T_{cc}(3875)^+$  [15, 16], composed of  $cs\bar{u}\bar{d}$  and  $cc\bar{u}\bar{d}$  quarks, respectively. Interestingly, most of these states have masses close to thresholds of hadron pairs, which may indicate that they are hadronic molecules loosely bound by nucleon-like meson-exchange forces [17–20]. There are a number of other possible explanations, including that these particles are compact multi-quark states [21–23], hadroquarkonia in which a  $c\bar{c}$  core is bound to light quarks and/or gluons via chromo-electric dipole forces [24], or cusps produced by near-threshold kinematics involving open-charm hadrons, or other dominant processes [25, 26].

The  $\chi_{c0}(3930)$  state was observed by the LHCb collaboration in the  $D^+D^-$  invariant-mass spectrum [14]. The mass and width of this state are consistent with those of the  $X(3915)$  resonance observed in the  $\omega J/\psi$  invariant-mass spectrum [27–30]. Moreover, the  $X(3915)$  also has preferred spin ( $J$ ), parity ( $P$ ), and charge-parity ( $C$ ) quantum numbers of  $J^{PC} = 0^{++}$  [30, 31], so the two states are treated as a single state in the following discussions unless otherwise specified. However, the  $\chi_{c0}(3930)$  state is not considered to be consistent with being a candidate for either the  $\chi_{c0}(2P)$  or  $\chi_{c0}(3P)$  state [32–36]. Lebed *et al.* [37] propose that it is the lightest  $c\bar{c}s\bar{s}$  state. Calculations based on QCD sum rules [38] favour the  $\chi_{c0}(3930)$  state as a  $0^{++}$   $[cq][\bar{c}\bar{q}]$  (where  $q = u, d$ ) or  $[cs][\bar{c}\bar{s}]$  tetraquark. Recent lattice QCD results also indicate that this state is dominated by the  $c\bar{c}s\bar{s}$  constituents [39]. The  $D_s^+D_s^-$  molecular interpretation is also possible, as suggested by the quark delocalization color-screening model [40] and phenomenological studies [41, 42]. All these developments point to a potential resonant structure in the vicinity of the threshold in the  $D_s^+D_s^-$  invariant-mass spectrum.

Previously, only the Belle experiment analysed the  $D_s^+D_s^-$  invariant-mass spectrum in processes involving initial-state radiation, where only  $1^{--}$  charmonium(-like) states can contribute [43]. The  $B^+ \rightarrow D_s^+D_s^-K^+$  process, given its large branching fraction measured in the accompanying paper [44], provides a good opportunity to study resonances in the  $D_s^+D_s^-$  final states, both scalars and those of higher spin, such as the  $0^{++}$  charmonium(-like) states  $\chi_{c0}(4500)$  and  $\chi_{c0}(4700)$  possibly having intrinsic  $c\bar{c}s\bar{s}$  component [12], the well-known  $1^{--}$  charmonium states, such as  $\psi(4040)$ ,  $\psi(4160)$ ,  $\psi(4260)$ ,  $\psi(4415)$  and  $\psi(4660)$  [31, 45, 46].

In this Letter an amplitude analysis of about 360 reconstructed  $B^+ \rightarrow D_s^+D_s^-K^+$  signal decays is presented, leading to the first observation of a near-threshold peaking structure in the  $D_s^+D_s^-$  system, denoted by  $X(3960)$ . This analysis is based on proton-proton ( $pp$ ) collision data collected by the LHCb experiment at centre-of-mass energies of 7, 8 and 13 TeV between 2011 and 2018, corresponding to an integrated luminosity of  $9 \text{ fb}^{-1}$ . The details of the detector, data and simulation, selection criteria, background composition and  $B^+$  invariant-mass fit can be found in the accompanying paper [44].

To improve the resolution on the masses of the two-body combinations that are used in

<sup>1</sup>Hadrons that are not classified as mesons or baryons are collectively called exotic hadrons.

<sup>2</sup>The inclusion of charge-conjugate processes is always implied and natural units with  $\hbar = c = 1$  are used throughout the Letter, unless otherwise noted.

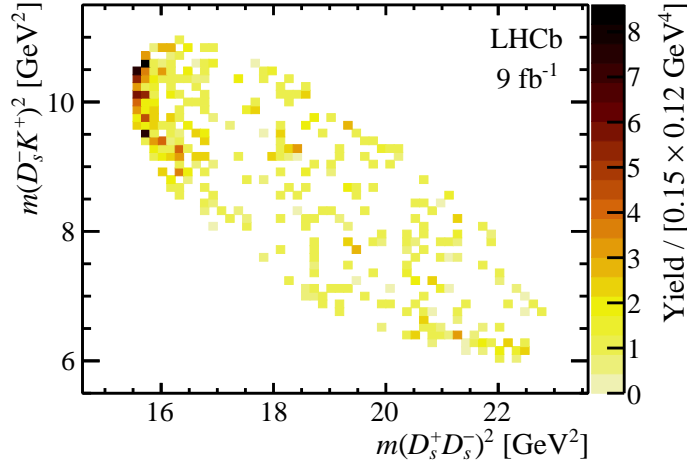


Figure 1: Dalitz-plot distribution for the  $B^+ \rightarrow D_s^+ D_s^- K^+$  decay after background subtraction.

the amplitude analysis, the four momentum of each final-state particle is determined from a kinematic fit [47] where the  $B^+$  mass is constrained to its known value [31]. Figure 1 shows the resulting Dalitz-plot distribution for the  $B^+ \rightarrow D_s^+ D_s^- K^+$  signal decays as a function of the  $D_s^+ D_s^-$  and  $D_s^- K^+$  invariant masses squared, where the non- $B^+$  background is subtracted by the *sPlot* technique [48]. The most evident feature is the band near the  $D_s^+ D_s^-$  threshold. To validate that this peaking structure is not due to the combinatorial background, the  $D_s^+ D_s^-$  invariant-mass distribution of candidates in the mass region above the  $B^+$  peak is investigated and no peak is observed.

Employing an unbinned maximum-likelihood method, a full amplitude fit with the *sFit* technique [49] is performed to investigate the intermediate states and determine the quantum numbers  $J^{PC}$  of any new particle. Two known  $1^{--}$  charmonium states,  $\psi(4260)$  and  $\psi(4660)$  [31, 45, 46], and two new  $0^{++}$   $X$  states are needed to fit the structures in the  $D_s^+ D_s^-$  spectrum. One of these scalars,  $X(3960)$ , describes the  $D_s^+ D_s^-$  threshold enhancement and the other, designated  $X_0(4140)$ , is necessary to model the dip around 4140 MeV, as shown in Fig. 2. The subscript 0 is used to distinguish this structure from the  $1^{++}$   $X(4140)$  state seen in the  $J/\psi\phi$  final state [31]. Additionally, an  $S$ -wave three-body phase-space function [31] is employed to model the nonresonant (NR)  $B^+ \rightarrow D_s^+ D_s^- K^+$  component. Since no significant contribution of any state is observed in either the  $D_s^- K^+$  or  $D_s^+ K^+$  systems, these five contributions constitute the baseline model.

The helicity formalism [50] is used to construct the amplitude model of the  $B^+ \rightarrow D_s^+ D_s^- K^+$  decay, with a similar approach applied to previous LHCb analyses of  $B^+$  and  $B_s^0$  decays to three pseudoscalar particles [14, 51–53]. The resonant structure near the  $D_s^+ D_s^-$  mass threshold is parameterised by a Flatté-like function [19, 31, 54] depending on the invariant mass  $m$

$$R(m | M_0, g_j) = \frac{1}{M_0^2 - m^2 - iM_0 \sum_j g_j \rho_j(m)}, \quad (1)$$

where  $M_0$  is the mass of the resonance,  $g_j$  denotes the coupling of this resonance to the  $j$ -th channel,  $\rho_j(m)$  is the phase-space factor [31] for the  $j$ -th two-body decay. When the value of  $m$  is below the threshold of the channel  $j$ , *i.e.*  $q_j^2 < 0$ , the analytic continuation

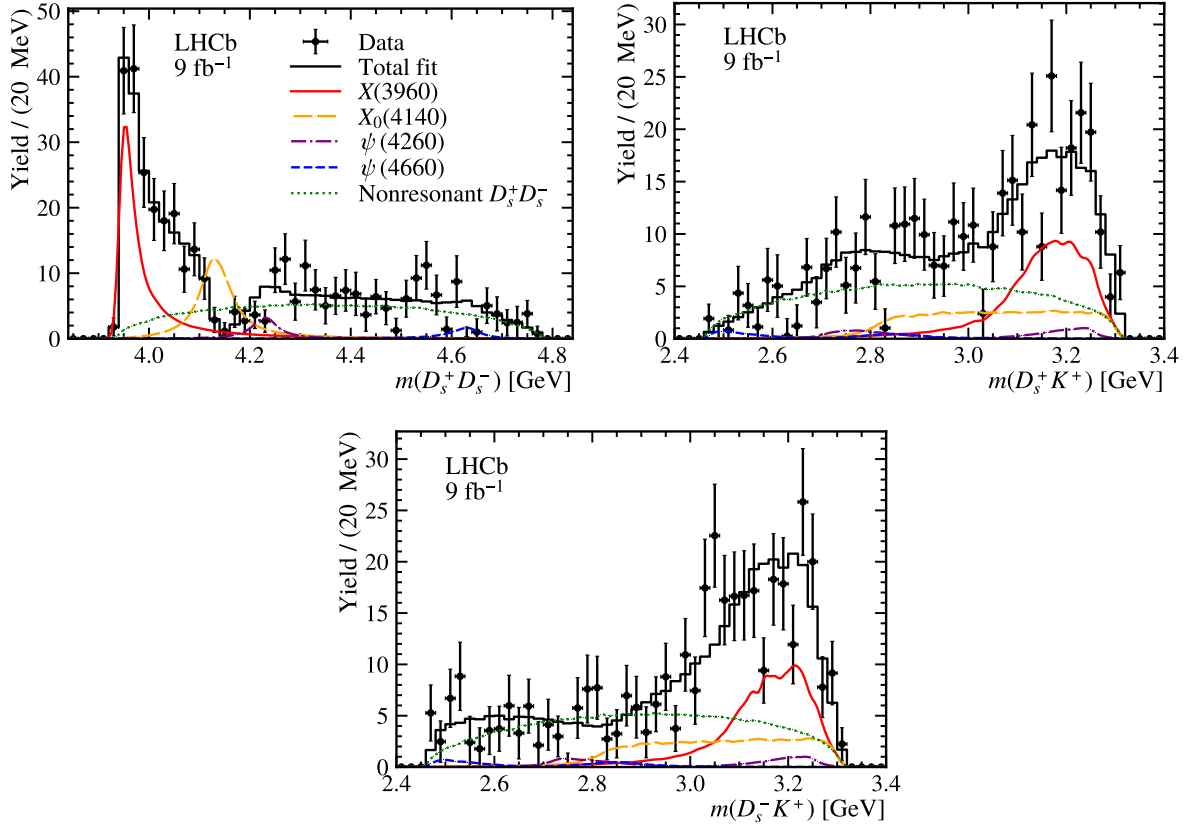


Figure 2: Background-subtracted invariant-mass distributions (top left)  $m(D_s^+ D_s^-)$ , (top right)  $m(D_s^+ K^+)$  and (bottom)  $m(D_s^- K^+)$  for the  $B^+ \rightarrow D_s^+ D_s^- K^+$  signal. The projections of the fit with the baseline amplitude model are also shown.

is applied for  $q_j = i\sqrt{-q_j^2}$  [54, 55]. The total width of the resonance is calculated as  $\Gamma_0 = \sum_j g_j \rho_j(M_0)$ . In the baseline model, only the  $D_s^+ D_s^-$  channel is included in the Flatté-like parameterisation.

Other resonances are modelled by a relativistic Breit–Wigner function  $\text{BW}(m | M_0, \Gamma_0)$  with a mass-dependent width [31]. The radius of each resonance entering the Blatt–Weisskopf barrier factor [56–58] is set to  $3 \text{ GeV}^{-1}$ , corresponding to about 0.6 fm.

The total probability density function is the squared modulus of the total decay amplitude multiplied by the efficiency, normalised to ensure that the integral over the Dalitz plot is unity. The fit fraction  $\mathcal{F}_i$  expresses the fraction of the total rate due to component  $i$ , and the interference fraction  $\mathcal{I}_{ij}$  describes the interference between components  $i$  and  $j$ . They are defined in Eqs. (18) and (19) of Ref. [52], such that  $\sum_i \mathcal{F}_i + \sum_{i < j} \mathcal{I}_{ij} = 1$ .

As shown in Fig. 2, the two-body mass distributions are well modelled by the baseline amplitude fit. The corresponding numerical results are summarised in Table 1, including the mass, width, fit fraction, and significance ( $\mathcal{S}$ ) of each component. The significance of a given component is evaluated by assuming that the change of twice the negative log-likelihood ( $-2 \ln \mathcal{L}$ ) between the baseline fit and the fit without that component obeys a  $\chi^2$  distribution, where the number of degrees of freedom (n.d.f.) is given by the change in the number of free parameters. All the components included in the baseline

Table 1: Summary of the main results obtained with the baseline model, where the first uncertainty is statistical and the second systematic. The last column shows the signal significance with (without) the systematic uncertainty included.

Component	$J^{PC}$	$M_0$ (MeV)	$\Gamma_0$ (MeV)	$\mathcal{F}$ (%)	$\mathcal{S}$ ( $\sigma$ )
$X(3960)$	$0^{++}$	$3956 \pm 5 \pm 10$	$43 \pm 13 \pm 8$	$25.4 \pm 7.7 \pm 5.0$	12.6 (14.6)
$X_0(4140)$	$0^{++}$	$4133 \pm 6 \pm 6$	$67 \pm 17 \pm 7$	$16.7 \pm 4.7 \pm 3.9$	3.8 (4.1)
$\psi(4260)$	$1^{--}$	4230 [59]	55 [59]	$3.6 \pm 0.4 \pm 3.2$	3.2 (3.6)
$\psi(4660)$	$1^{--}$	4633 [31]	64 [31]	$2.2 \pm 0.2 \pm 0.8$	3.0 (3.2)
NR	$0^{++}$	-	-	$46.1 \pm 13.2 \pm 11.3$	3.1 (3.4)

model have a statistical significance higher than three standard deviations ( $\sigma$ ), where the  $X(3960)$  and  $X_0(4140)$  states are found to be  $14.6\sigma$  and  $4.1\sigma$  significant, respectively. The obtained significances for the  $X(3960)$  and  $X_0(4140)$  resonances are also validated using pseudoexperiments.

The  $J^{PC}$  assignment for the system of a pair of oppositely-charged pseudoscalar mesons must be in the series  $0^{++}$ ,  $1^{--}$ ,  $2^{++}$ , etc. States with higher intrinsic spin are not expected to contribute significantly in the current dataset. To determine the  $X(3960)$  quantum numbers, fits with the baseline model are performed under alternative  $J^{PC}$  hypotheses,  $1^{--}$ ,  $2^{++}$ , instead of  $0^{++}$ . The significance to reject a  $J^{PC}$  hypothesis is computed as  $\sqrt{\Delta(-2\ln\mathcal{L})}$ , where  $\Delta(-2\ln\mathcal{L}) = -(2\ln\mathcal{L}(0^{++}) - 2\ln\mathcal{L}(J^{PC}))$ , and indicates the likelihood difference between the fits for the preferred  $0^{++}$  assignment and for each alternative  $J^{PC}$  hypothesis. To ensure that for different  $J^{PC}$  hypotheses this resonance corresponds to the same particle, the mass and the width are limited to be within a  $\pm 3\sigma$  range of the baseline fit results. The  $0^{++}$  assignment is preferred over  $1^{--}$  and  $2^{++}$  hypotheses by  $9.3\sigma$  and  $12.3\sigma$ , respectively. Similarly, replacing the baseline  $0^{++}$  assignment by  $1^{--}$  or  $2^{++}$  for the  $X_0(4140)$  state deteriorates the fit quality. The  $0^{++}$  assignment is favoured over  $1^{--}$  ( $2^{++}$ ) hypothesis at a  $3.5\sigma$  ( $4.2\sigma$ ) level. Within the baseline model this  $0^{++}$  state produces the dip around 4140 MeV via destructive interference with the  $0^{++}$  NR and  $X(3960)$  components, with the interference fractions of, respectively,  $(-22.4 \pm 6.4)\%$  and  $(-5.2 \pm 3.9)\%$ , where the uncertainties are statistical only.

Systematic uncertainties on the measured resonance properties are evaluated, and are summarised in Table S1 in the supplemental material [60]. Corrections, derived from calibration samples, are applied to account for possible discrepancies between data and simulation in the hardware trigger and particle-identification responses. The uncertainty due to the limited size of the simulation samples is evaluated using the bootstrap method [61]. Additional resonances, not included in the baseline model (states in the  $D_s^+ D_s^-$  system:  $0^{++}$   $\chi_{c0}(4500)$  and  $\chi_{c0}(4700)$  [12],  $1^{--}$   $\psi(4040)$ ,  $\psi(4160)$  and  $\psi(4415)$  [31], and  $2^{++}$   $\chi_{c2}(3930)$  [14]; and in the  $D_s^- K^+$  system:  $0^+$   $\bar{D}_0^*(2300)^0$  [31],  $1^-$   $\bar{D}_1^*(2600)^0$  [31, 62] and  $\bar{D}_1^*(2760)^0$  [63], and  $2^+$   $\bar{D}_2^*(2460)^0$  [31]) are utilised to estimate the uncertainty due to insufficient consideration of possible amplitude components. None of these states significantly improve the baseline model. The  $c\bar{c}s\bar{s}$  candidates  $\chi_{c0}(4500)$  and  $\chi_{c0}(4700)$  have statistical significances of  $0.8\sigma$  and  $1.3\sigma$ , respectively, and their fit fractions are  $(0.6 \pm 1.0)\%$  and  $(2.4 \pm 1.8)\%$ , where the uncertainties are statistical. The Blatt–Weisskopf hadron size is varied between 1.5 and 4.5  $\text{GeV}^{-1}$ . The fixed masses and

widths of two baseline  $\psi$  states are varied by their corresponding uncertainties. The Flatté-like parameterisation for the  $X(3960)$  state is replaced by a constant-width relativistic Breit–Wigner function. The uncertainty due to the possible bias of the *sFit* method is evaluated using pseudoexperiments. The total systematic uncertainties on mass, width, and fit fraction are obtained by adding all contributions in quadrature, assuming that each source is independent. Regarding the total significance for each component in the baseline model, the smallest significance among these systematic tests is selected.

The measured mass and width of the  $X(3960)$  state are consistent with those of the  $\chi_{c0}(3930)$  meson [14] within  $3\sigma$ . Assuming that the  $X(3960)$  in the  $D_s^+D_s^-$  system and the  $\chi_{c0}(3930)$  in the  $D^+D^-$  system are the same state, the baseline model is extended by adding a second channel ( $D^+D^-$ ) in the Flatté-like parameterisation. The corresponding fit projections and numerical results can be found in the supplemental material [60]. The likelihood is essentially unchanged while the n.d.f. is increased by one compared to the baseline fit. The coupling strength of the  $X(3960)$  state to  $D_s^+D_s^-$  ( $D^+D^-$ ) is found to be  $0.33 \pm 1.18$  ( $0.15 \pm 0.33$ ) GeV. The masses and fit fractions of all components are consistent with those in the baseline one-channel Flatté-like model.

In the case that the  $X(3960)$  and  $\chi_{c0}(3930)$  states are the same particle, the partial width ratio of such an  $X$  resonance decaying to  $D_s^+D_s^-$  and  $D^+D^-$  final states is calculated as

$$\frac{\Gamma(X \rightarrow D^+D^-)}{\Gamma(X \rightarrow D_s^+D_s^-)} = \frac{\mathcal{B}^{(1)} \mathcal{F}_X^{(1)}}{\mathcal{B}^{(2)} \mathcal{F}_X^{(2)}} = 0.29 \pm 0.09 \pm 0.10 \pm 0.08, \quad (2)$$

where the superscripts (1) and (2) indicate the  $B^+ \rightarrow D^+D^-K^+$  and  $B^+ \rightarrow D_s^+D_s^-K^+$  channels, respectively,  $\mathcal{F}_X^{(1)} = (3.70 \pm 0.92)\%$  is the fit fraction of the  $\chi_{c0}(3930)$  state in the  $B^+ \rightarrow D^+D^-K^+$  decay [14],  $\mathcal{F}_X^{(2)}$  is the fit fraction of the  $X(3960)$  resonance presented in this Letter, and the branching fraction ratio  $\mathcal{B}^{(1)}/\mathcal{B}^{(2)}$  is taken from the accompanying paper [44]. The first uncertainty is statistical, the second systematic, and the third is due to uncertainties in the measured branching fractions,  $\mathcal{B}(D^+ \rightarrow K^-\pi^+\pi^+)$  and  $\mathcal{B}(D_s^+ \rightarrow K^-K^+\pi^+)$  [31], and the uncertainty on  $\mathcal{F}_X^{(1)}$  [14]. This ratio is compatible with that of the couplings mentioned above.

It is well known that the creation of an  $s\bar{s}$  quark pair from the vacuum is suppressed relative to  $u\bar{u}$  or  $d\bar{d}$  pairs. Moreover, the  $X \rightarrow D_s^+D_s^-$  decay, occurring near the threshold, has a rather smaller phase-space factor than that of  $X \rightarrow D^+D^-$ . These two features indicate that  $\Gamma(X \rightarrow D^+D^-)$  should be considerably larger than  $\Gamma(X \rightarrow D_s^+D_s^-)$  if  $X$  does not have any intrinsic  $s\bar{s}$  content. However, the value measured in Eq. (2) contradicts this expectation. This implies that the  $X(3960)$  and  $\chi_{c0}(3930)$  are either not the same resonance, or they are the same non-conventional charmonium-like state, for instance, a candidate containing the dominant  $c\bar{c}s\bar{s}$  constituents predicted in recent theoretical models [37–42, 64].

There is no obvious candidate within conventional charmonium multiplets for  $X(3960)$  or  $\chi_{c0}(3930)$  assignment. First of all, the mass of the  $\chi_{c0}(3930)$  state is far from predictions for the  $\chi_{c0}(3P)$ , which lies within the range 4131–4292 MeV [32, 34]. For the  $\chi_{c0}(2P)$  state most potential models predict mass in the range 3842–3868 MeV [33–35], except the Godfrey-Isgur model which gives 3916 MeV [32]. Second, the  $\chi_{c0}(3930)$  state interpreted as  $\chi_{c0}(2P)$  would give too small a mass splitting with respect to the  $\chi_{c2}(3930)$  state [14] identified as  $\chi_{c2}(2P)$  [32–35]. In addition, interpreting the  $\chi_{c0}(3930)$  state as

the  $\chi_{c0}(2P)$  charmonium would result in inconsistent decay widths, as the Okubo-Zweig-Iizuka (OZI) [65, 66] suppressed channel  $\chi_{c0}(3930) \rightarrow \omega J/\psi$  has decay width larger than theoretical expectations, whereas the  $S$ -wave OZI-allowed  $\chi_{c0}(3930) \rightarrow D\bar{D}$  mode has smaller decay width than the expectations [35, 36]. As a consequence, neither the  $X(3960)$  nor the  $\chi_{c0}(3930)$  is likely to be a pure  $\chi_{c0}(2P)$  or  $\chi_{c0}(3P)$  charmonium state.

To test the possibility that the dip in the  $D_s^+ D_s^-$  invariant mass around 4140 MeV can be produced by the opening of the nearby  $J/\psi\phi$  threshold, without introducing an additional resonance, we employ a simple  $K$ -matrix model that contains the single resonance  $X(3960)$  and two coupled channels,  $D_s^+ D_s^-$  and  $J/\psi\phi$ . The  $K$ -matrix reads

$$\begin{pmatrix} \mathcal{K}_{D_s^+ D_s^- \rightarrow D_s^+ D_s^-} & \mathcal{K}_{D_s^+ D_s^- \rightarrow J/\psi\phi} \\ \mathcal{K}_{J/\psi\phi \rightarrow D_s^+ D_s^-} & \mathcal{K}_{J/\psi\phi \rightarrow J/\psi\phi} \end{pmatrix} \equiv \begin{pmatrix} \mathcal{K}_{11} & \mathcal{K}_{12} \\ \mathcal{K}_{21} & \mathcal{K}_{22} \end{pmatrix}, \quad (3)$$

where  $\mathcal{K}_{12} = \mathcal{K}_{21}$ , and the subscripts 1 and 2 represent  $D_s^+ D_s^-$  and  $J/\psi\phi$  final states, respectively. One possible choice for the  $2 \times 2$   $K$ -matrix parameterisation [31] is

$$\mathcal{K}_{ba}(m) = \sum_R \frac{g_b^R g_a^R}{M_R^2 - m^2} + f_{ba}, \quad (4)$$

where  $M_R$  refers to the bare mass of the resonance  $R$ ,  $m$  is the  $D_s^+ D_s^-$  invariant mass,  $g_a^R$  denotes the bare coupling of the resonance  $R$  to the channel  $a$ , and the  $f_{ba}$  is a real matrix parameterising the non-pole part of the  $K$ -matrix. As the  $X(3960)$  mass is about 160 MeV lower than the  $J/\psi\phi$  threshold and its width is less than 50 MeV, the coupling of the  $X(3960)$  state to  $J/\psi\phi$  should be negligible, giving  $g_2^R = 0$ . This results in the  $X(3960)$  resonance entering the  $\mathcal{K}_{11}$  element only. The production amplitude is expressed in the  $P$ -vector formalism [31, 67, 68], which gives

$$\mathcal{P}_b(m) = \sum_R \frac{\beta_R g_b^R}{M_R^2 - m^2} + \beta_b, \quad (5)$$

where  $\beta_R$  and  $\beta_b$  are complex free parameters due to rescattering effects or missing channels [59]. The amplitude  $\mathcal{M}$  is

$$\mathcal{M}_a = \sum_b (I - i\rho\mathcal{K})_{ab}^{-1} \mathcal{P}_b, \quad (6)$$

where  $\rho = \text{diag}\{\rho_{11}, \rho_{22}\}$  is the diagonal matrix composed of phase-space factors,  $I$  represents the identity matrix, and  $a = 1$  for the  $D_s^+ D_s^-$  channel under consideration.

The fit demonstrates that the dip around the  $J/\psi\phi$  threshold can also be modelled by the  $J/\psi\phi \rightarrow D_s^+ D_s^-$  rescattering, and results in a  $-2 \ln \mathcal{L}$  that is worse by 6.0, while the n.d.f. is increased by one, compared to the baseline fit. The fit projections and numerical results can be found in the supplemental material [60]. Since the fit quality of the  $K$ -matrix parameterisation is close to that of the baseline model, a strong conclusion cannot be drawn whether the dip is due to destructive interference with the  $X_0(4140)$  resonance or caused by the  $J/\psi\phi \rightarrow D_s^+ D_s^-$  rescattering.

In addition, it is found that the fits with the two-channel Flatté-like and  $K$ -matrix parameterisations are unstable, due to having too many free parameters for the limited sample size. Consequently, the statistical uncertainties for some parameters are large. Therefore, neither of these parameterisations are taken as the baseline model.



In conclusion, the first amplitude analysis of the  $B^+ \rightarrow D_s^+ D_s^- K^+$  decay is performed using  $pp$  collision data with an integrated luminosity of  $9 \text{ fb}^{-1}$  collected by the LHCb experiment between 2011 and 2018. A peaking structure near the  $D_s^+ D_s^-$  mass threshold, denoted as  $X(3960)$ , is observed with a significance larger than  $12\sigma$ . Its quantum numbers are determined to be  $J^{PC} = 0^{++}$ , favoured over  $1^{--}$  or  $2^{++}$  with a significance greater than  $9\sigma$ . As argued above, the  $X(3960)$  and  $\chi_{c0}(3930)$  states are unlikely to be the same pure conventional charmonium state. The  $X(3960)$  resonance presented in this Letter is a candidate for an exotic state predominantly consisting of  $c\bar{c}s\bar{s}$  constituents, as suggested in recent theoretical literature [37–42, 64]. If predominant  $c\bar{c}s\bar{s}$  content is confirmed, this state should be labelled  $T_{\psi\phi}^f(3960)$  in the new naming scheme for exotic hadrons [69]. In addition, a dip around 4140 MeV can be described either by a  $0^{++}$   $X_0(4140)$  resonance having a significance of  $3.7\sigma$ , or the coupled-channel effect of the  $J/\psi\phi \leftrightarrow D_s^+ D_s^-$  reaction. The data from the forthcoming Run 3 of the LHCb experiment and from the Belle II experiment will be critical to clarify the nature of these phenomena.

# Supplemental material

Table S1: Summary of the systematic uncertainties on the parameters measured in the amplitude analysis. Mass ( $M_0$ ) and width ( $\Gamma_0$ ) are in units of MeV, while fit fraction ( $\mathcal{F}$ ) is in %.

Source	X(3960)			X <sub>0</sub> (4140)			$\psi(4260)$	$\psi(4660)$	NR
	$M_0$	$\Gamma_0$	$\mathcal{F}$	$M_0$	$\Gamma_0$	$\mathcal{F}$	$\mathcal{F}$	$\mathcal{F}$	$\mathcal{F}$
Trigger	0	0	0.6	0	0	0.1	0.0	0.0	0.7
Simulation sample size	2	1	0.7	1	1	0.5	0.0	0.0	1.7
Particle identification	0	0	0.5	0	2	0.0	0.0	0.0	0.7
Additional fit components	1	3	3.4	3	5	2.5	3.2	0.7	10.1
Hadron size	0	1	0.0	1	1	0.1	0.0	0.0	0.1
Fixed parameters	1	2	2.8	4	4	2.9	0.1	0.1	3.7
X(3960) model	10	7	1.6	0	1	0.7	0.0	0.0	2.1
<i>sFit</i> bias	1.9	1.5	1.5	2.6	1.1	0.4	0.3	0.3	2.1
Total	10	8	5.0	6	7	3.9	3.2	0.8	11.3

Table S2: Main results found in two-channel Flatté-like parameterisation, where the coupling strength of the X(3960) state to  $D_s^+ D_s^-$  ( $D^+ D^-$ ) is obtained to be  $0.33 \pm 1.18$  ( $0.15 \pm 0.33$ ) GeV. Uncertainties are statistical only. The large uncertainty on  $\Gamma_0$  for the X(3960) state is due to the large uncertainty on the coupling strengths.

Contribution	$J^{PC}$	$M_0$ (MeV)	$\Gamma_0$ (MeV)	$\mathcal{F}$ (%)
X(3960)	$0^{++}$	$3951 \pm 14$	$38 \pm 104$	$25.0 \pm 7.6$
X <sub>0</sub> (4140)	$0^{++}$	$4133 \pm 7$	$67 \pm 16$	$16.7 \pm 4.6$
$\psi(4260)$	$1^{--}$	4230 [59]	55 [59]	$3.6 \pm 0.4$
$\psi(4660)$	$1^{--}$	4633 [31]	64 [31]	$2.2 \pm 0.2$
NR	$0^{++}$	-	-	$45.9 \pm 10.9$

Table S3: Main results found from the  $K$ -matrix fit. Uncertainties are statistical only.

Contribution	$J^{PC}$	$M_R$ (MeV)	$g_1^R$ (MeV)	$\Gamma_0$ (MeV)	$\mathcal{F}$ (%)
$ \mathcal{M}_1 ^2$	$0^{++}$	$3957 \pm 14$	$1350 \pm 344$		$94.7 \pm 0.4$
$\psi(4260)$	$1^{--}$	4230 [59]		55 [59]	$3.2 \pm 0.5$
$\psi(4660)$	$1^{--}$	4633 [31]		64 [31]	$2.1 \pm 0.2$
$\beta_R$		$(1, 0i)$	$\beta_1$	$(-1.2, 2.5i) \pm (4.5, 3.1i)$	
$\beta_2$		$(-137.2, -1.5i) \pm (2.7, 218.6i)$	$f_{11}$	$0.8 \pm 1.2$	
$f_{12} = f_{21}$		$0.1 \pm 0.1$	$f_{22}$	$8.0 \pm 5.1$	

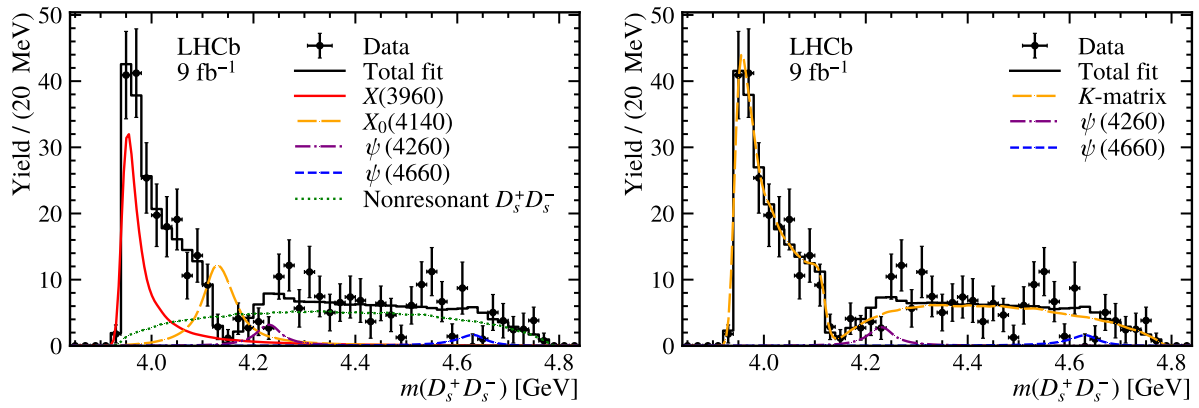


Figure S1: Background-subtracted distribution of the  $D_s^+ D_s^-$  invariant mass of  $B^+ \rightarrow D_s^+ D_s^- K^+$  decays with fit results obtained from (left) two-channel Flatté-like and (right)  $K$ -matrix parameterisations. The fit projections for the  $D_s^- K^+$  and  $D_s^+ K^+$  invariant-mass spectra look very similar to the baseline model.

## References

- [1] Belle collaboration, S. K. Choi *et al.*, *Observation of a resonance-like structure in the  $\pi^\pm\psi'$  mass distribution in exclusive  $B \rightarrow K\pi^\pm\psi'$  decays*, Phys. Rev. Lett. **100** (2008) 142001, arXiv:0708.1790.
- [2] Belle collaboration, K. Chilikin *et al.*, *Experimental constraints on the spin and parity of the  $Z(4430)^+$* , Phys. Rev. **D88** (2013) 074026, arXiv:1306.4894.
- [3] Belle collaboration, A. Bondar *et al.*, *Observation of two charged bottomonium-like resonances in  $\Upsilon(5S)$  decays*, Phys. Rev. Lett. **108** (2012) 122001, arXiv:1110.2251.
- [4] BESIII collaboration, M. Ablikim *et al.*, *Observation of a charged charmoniumlike structure in  $e^+e^- \rightarrow \pi^+\pi^-J/\psi$  at  $\sqrt{s} = 4.26$  GeV*, Phys. Rev. Lett. **110** (2013) 252001, arXiv:1303.5949.
- [5] Belle collaboration, Z. Q. Liu *et al.*, *Study of  $e^+e^- \rightarrow \pi^+\pi^-J/\psi$  and observation of a charged charmoniumlike state at Belle*, Phys. Rev. Lett. **110** (2013) 252002, Erratum *ibid.* **111** (2013) 019901, arXiv:1304.0121.
- [6] T. Xiao, S. Dobbs, A. Tomaradze, and K. K. Seth, *Observation of the charged hadron  $Z_c^\pm(3900)$  and evidence for the neutral  $Z_c^0(3900)$  in  $e^+e^- \rightarrow \pi\pi J/\psi$  at  $\sqrt{s} = 4170$  MeV*, Phys. Lett. B **727** (2013) 366, arXiv:1304.3036.
- [7] BESIII collaboration, M. Ablikim *et al.*, *Observation of a charged charmoniumlike structure in  $e^+e^- \rightarrow (D^*\bar{D}^*)^\pm\pi^\mp$  at  $\sqrt{s} = 4.26$  GeV*, Phys. Rev. Lett. **112** (2014) 132001, arXiv:1308.2760.
- [8] BESIII collaboration, M. Ablikim *et al.*, *Observation of a charged charmoniumlike structure  $Z_c(4020)$  and search for the  $Z_c(3900)$  in  $e^+e^- \rightarrow \pi^+\pi^-h_c$* , Phys. Rev. Lett. **111** (2013) 242001, arXiv:1309.1896.
- [9] LHCb collaboration, R. Aaij *et al.*, *Observation of  $J/\psi p$  resonances consistent with pentaquark states in  $\Lambda_b^0 \rightarrow J/\psi p K^-$  decays*, Phys. Rev. Lett. **115** (2015) 072001, arXiv:1507.03414.
- [10] LHCb collaboration, R. Aaij *et al.*, *Observation of a narrow pentaquark state,  $P_c(4312)^+$ , and of two-peak structure of the  $P_c(4450)^+$* , Phys. Rev. Lett. **122** (2019) 222001, arXiv:1904.03947.
- [11] BESIII collaboration, M. Ablikim *et al.*, *Observation of a near-threshold structure in the  $K^+$  recoil-mass spectra in  $e^+e^- \rightarrow K^+(D_s^- D^{*0} + D_s^{*-} D^0)$* , Phys. Rev. Lett. **126** (2021) 102001, arXiv:2011.07855.
- [12] LHCb collaboration, R. Aaij *et al.*, *Observation of new resonances decaying to  $J/\psi K^+$  and  $J/\psi \phi$* , Phys. Rev. Lett. **127** (2021) 082001, arXiv:2103.01803.
- [13] LHCb collaboration, R. Aaij *et al.*, *Model-independent study of structure in  $B^+ \rightarrow D^+ D^- K^+$  decays*, Phys. Rev. Lett. **125** (2020) 242001, arXiv:2009.00025.
- [14] LHCb collaboration, R. Aaij *et al.*, *Amplitude analysis of the  $B^+ \rightarrow D^+ D^- K^+$  decay*, Phys. Rev. **D102** (2020) 112003, arXiv:2009.00026.

- [15] LHCb collaboration, R. Aaij *et al.*, *Observation of an exotic narrow doubly charmed tetraquark*, Nature Phys. **18** (2022) 751, [arXiv:2109.01038](#).
- [16] LHCb collaboration, R. Aaij *et al.*, *Study of the doubly charmed tetraquark  $T_{cc}^+$* , Nature Commun. **13** (2022) 3351, [arXiv:2109.01056](#).
- [17] Q.-R. Gong *et al.*,  *$Z_c(3900)$  as a  $D\bar{D}^*$  molecule from the pole counting rule*, Phys. Rev. **D94** (2016) 114019, [arXiv:1604.08836](#).
- [18] Q.-R. Gong, J.-L. Pang, Y.-F. Wang, and H.-Q. Zheng, *The  $Z_c(3900)$  peak does not come from the “triangle singularity”*, Eur. Phys. J. **C78** (2018) 276, [arXiv:1612.08159](#).
- [19] Q.-F. Cao, H. Chen, H.-R. Qi, and H.-Q. Zheng, *Some remarks on  $X(6900)$* , Chin. Phys. **C45** (2021) 103102, [arXiv:2011.04347](#).
- [20] H. Chen, H.-R. Qi, and H.-Q. Zheng,  *$X_1(2900)$  as a  $\bar{D}_1 K$  molecule*, Eur. Phys. J. **C81** (2021) 812, [arXiv:2108.02387](#).
- [21] L. Maiani *et al.*, *A  $J^{PG} = 1^{++}$  charged resonance in the  $Y(4260) \rightarrow \pi^+\pi^- J/\psi$  decay?*, Phys. Rev. **D87** (2013) 111102, [arXiv:1303.6857](#).
- [22] J. M. Dias, F. S. Navarra, M. Nielsen, and C. M. Zanetti,  *$Z_c(3900)^+$  decay width in QCD sum rules*, Phys. Rev. **D88** (2013) 016004, [arXiv:1304.6433](#).
- [23] L. Maiani, F. Piccinini, A. D. Polosa, and V. Riquer, *Diquark-antidiquarks with hidden or open charm and the nature of  $X(3872)$* , Phys. Rev. **D71** (2005) 014028, [arXiv:hep-ph/0412098](#).
- [24] M. Alberti *et al.*, *Hadroquarkonium from lattice QCD*, Phys. Rev. **D95** (2017) 074501, [arXiv:1608.06537](#).
- [25] D. V. Bugg, *An Explanation of Belle states  $Z_b(10610)$  and  $Z_b(10650)$* , EPL **96** (2011) 11002, [arXiv:1105.5492](#).
- [26] F.-K. Guo, X.-H. Liu, and S. Sakai, *Threshold cusps and triangle singularities in hadronic reactions*, Prog. Part. Nucl. Phys. **112** (2020) 103757, [arXiv:1912.07030](#).
- [27] Belle collaboration, K. Abe *et al.*, *Observation of a near-threshold  $\omega J/\psi$  mass enhancement in exclusive  $B \rightarrow K\omega J/\psi$  decays*, Phys. Rev. Lett. **94** (2005) 182002, [arXiv:hep-ex/0408126](#).
- [28] BaBar collaboration, P. del Amo Sanchez *et al.*, *Evidence for the decay  $X(3872) \rightarrow J/\psi\omega$* , Phys. Rev. **D82** (2010) 011101, [arXiv:1005.5190](#).
- [29] Belle collaboration, S. Uehara *et al.*, *Observation of a charmonium-like enhancement in the  $\gamma\gamma \rightarrow \omega J/\psi$  process*, Phys. Rev. Lett. **104** (2010) 092001, [arXiv:0912.4451](#).
- [30] BaBar collaboration, J. P. Lees *et al.*, *Study of  $X(3915) \rightarrow J/\psi\omega$  in two-photon collisions*, Phys. Rev. **D86** (2012) 072002, [arXiv:1207.2651](#).
- [31] Particle Data Group, P. A. Zyla *et al.*, *Review of particle physics*, Prog. Theor. Exp. Phys. **2020** (2020) 083C01.

- [32] T. Barnes, S. Godfrey, and E. S. Swanson, *Higher charmonia*, Phys. Rev. **D72** (2005) 054026, [arXiv:hep-ph/0505002](#).
- [33] S. F. Radford and W. W. Repko, *Potential model calculations and predictions for heavy quarkonium*, Phys. Rev. **D75** (2007) 074031, [arXiv:hep-ph/0701117](#).
- [34] B.-Q. Li and K.-T. Chao, *Higher charmonia and X, Y, Z states with screened potential*, Phys. Rev. **D79** (2009) 094004, [arXiv:0903.5506](#).
- [35] H. Wang, Y. Yang, and J. Ping, *Strong decays of  $\chi_{cJ}(2P)$  and  $\chi_{cJ}(3P)$* , Eur. Phys. J. **A50** (2014) 76.
- [36] F.-K. Guo and U.-G. Meissner, *Where is the  $\chi_{c0}(2P)$ ?*, Phys. Rev. **D86** (2012) 091501, [arXiv:1208.1134](#).
- [37] R. F. Lebed and A. D. Polosa,  $\chi_{c0}(3915)$  *As the lightest  $c\bar{c}s\bar{s}$  state*, Phys. Rev. **D93** (2016) 094024, [arXiv:1602.08421](#).
- [38] W. Chen *et al.*, *Mass spectra for  $qc\bar{q}\bar{c}$ ,  $sc\bar{s}\bar{c}$ ,  $qb\bar{q}\bar{b}$ ,  $sb\bar{s}\bar{b}$ , tetraquark states with  $J^{PC} = 0^{++}$  and  $2^{++}$* , Phys. Rev. **D96** (2017) 114017, [arXiv:1706.09731](#).
- [39] S. Prelovsek *et al.*, *Charmonium-like resonances with  $J^{PC} = 0^{++}, 2^{++}$  in coupled  $D\bar{D}$ ,  $D_s\bar{D}_s$  scattering on the lattice*, JHEP **06** (2021) 035, [arXiv:2011.02542](#).
- [40] X. Liu *et al.*, *The explanation of some exotic states in the  $c\bar{c}s\bar{s}$  tetraquark system*, Eur. Phys. J. **C81** (2021) 950, [arXiv:2103.12425](#).
- [41] L. Meng, B. Wang, and S.-L. Zhu, *Predicting the  $\bar{D}_s^{(*)}D_s^{(*)}$  bound states as the partners of  $X(3872)$* , Sci. Bull. **66** (2021) 1288, [arXiv:2012.09813](#).
- [42] X.-K. Dong, F.-K. Guo, and B.-S. Zou, *A survey of heavy-antiheavy hadronic molecules*, Progr. Phys. **41** (2021) 65, [arXiv:2101.01021](#).
- [43] Belle collaboration, G. Pakhlova *et al.*, *Measurement of  $e^+e^- \rightarrow D_s^{(*)+}D_s^{(*)-}$  cross sections near threshold using initial-state radiation*, Phys. Rev. **D83** (2011) 011101, [arXiv:1011.4397](#).
- [44] LHCb collaboration, R. Aaij *et al.*, *First observation of the  $B^+ \rightarrow D_s^+D_s^-K^+$  decay*, LHCb-PAPER-2022-019, in preparation.
- [45] Q.-F. Cao *et al.*, *On leptonic width of  $X(4260)$* , Eur. Phys. J. **C81** (2021) 83, [arXiv:2002.05641](#).
- [46] Q.-F. Cao, H.-R. Qi, Y.-F. Wang, and H.-Q. Zheng, *Discussions on the line-shape of the  $X(4660)$  resonance*, Phys. Rev. **D100** (2019) 054040, [arXiv:1906.00356](#).
- [47] W. D. Hulsbergen, *Decay chain fitting with a Kalman filter*, Nucl. Instrum. Meth. **A552** (2005) 566, [arXiv:physics/0503191](#).
- [48] M. Pivk and F. R. Le Diberder, *sPlot: A statistical tool to unfold data distributions*, Nucl. Instrum. Meth. **A555** (2005) 356, [arXiv:physics/0402083](#).

- [49] Y. Xie, *sFit: a method for background subtraction in maximum likelihood fit*, arXiv:0905.0724.
- [50] S. U. Chung, *Spin formalisms*, CERN-71-08; J. D. Richman, *An experimenter's guide to the helicity formalism*, CALT-68-1148; M. Jacob and G. C. Wick, *On the general theory of collisions for particles with spin*, Annals Phys. **7** (1959) 404.
- [51] LHCb collaboration, R. Aaij *et al.*, *Dalitz plot analysis of  $B_s^0 \rightarrow \bar{D}^0 K^- \pi^+$  decays*, Phys. Rev. **D90** (2014) 072003, arXiv:1407.7712.
- [52] LHCb collaboration, R. Aaij *et al.*, *Amplitude analysis of  $B^- \rightarrow D^+ \pi^- \pi^-$  decays*, Phys. Rev. **D94** (2016) 072001, arXiv:1608.01289.
- [53] LHCb collaboration, R. Aaij *et al.*, *Amplitude analysis of the  $B^+ \rightarrow \pi^+ \pi^+ \pi^-$  decay*, Phys. Rev. **D101** (2020) 012006, arXiv:1909.05211.
- [54] S. M. Flatté, *Coupled-channel analysis of the  $\pi\eta$  and  $K\bar{K}$  systems near  $K\bar{K}$  threshold*, Phys. Lett. **B63** (1976) 224.
- [55] V. V. Anisovich and A. V. Sarantsev, *K-matrix analysis of the  $(IJ^{PC} = 00^{++})$ -wave in the mass region below 1900 MeV*, Eur. Phys. J. **A16** (2003) 229, arXiv:hep-ph/0204328.
- [56] J. M. Blatt and V. F. Weisskopf, *Theoretical nuclear physics*, Springer, New York, 1952.
- [57] F. Von Hippel and C. Quigg, *Centrifugal-barrier effects in resonance partial decay widths, shapes, and production amplitudes*, Phys. Rev. **D5** (1972) 624.
- [58] S. U. Chung *et al.*, *Partial wave analysis in K matrix formalism*, Annalen Phys. **4** (1995) 404.
- [59] Particle Data Group, M. Tanabashi *et al.*, *Review of particle physics*, Phys. Rev. **D98** (2018) 030001.
- [60] *See Supplemental material for a summary of systematic uncertainties, and main results and fit projections from both two-channel Flatté-like parameterisation and K-matrix model.*
- [61] B. Efron, *Bootstrap methods: Another look at the jackknife*, Ann. Statist. **7** (1979) 1.
- [62] LHCb collaboration, R. Aaij *et al.*, *Determination of quantum numbers for several excited charmed mesons observed in  $B^- \rightarrow D^{*+} \pi^- \pi^-$  decays*, Phys. Rev. **D101** (2020) 032005, arXiv:1911.03326.
- [63] LHCb collaboration, R. Aaij *et al.*, *First observation and amplitude analysis of the  $B^- \rightarrow D^+ K^- \pi^-$  decay*, Phys. Rev. **D91** (2015) 092002, Erratum *ibid.* **D93** (2016) 119901, arXiv:1503.02995.
- [64] E. Wang, W.-H. Liang, and E. Oset, *Analysis of the  $e^+e^- \rightarrow J/\psi D\bar{D}$  reaction close to the threshold concerning claims of a  $\chi_{c0}(2P)$  state*, Eur. Phys. J. **A57** (2021) 38, arXiv:1902.06461.

- [65] S. Okubo,  *$\Phi$  meson and unitary symmetry model*, Phys. Lett. **5** (1963) 165.
- [66] J. Iizuka, *Systematics and phenomenology of meson family*, Prog. Theor. Phys. Suppl. **37** (1966) 21.
- [67] I. J. R. Aitchison, *The K-matrix formalism for overlapping resonances*, Nucl. Phys. **A189** (1972) 417.
- [68] I. J. R. Aitchison, *Unitarity, analyticity and crossing symmetry in two- and three-hadron final state interactions*, arXiv:1507.02697.
- [69] LHCb collaboration, T. Gershon, *Exotic hadron naming convention*, arXiv:2206.15233.